Holzforschung, Vol. 61, pp. 582–588, 2007 • Copyright © by Walter de Gruyter • Berlin • New York. DOI 10.1515/HF.2007.089

Fracture characterisation of yew (*Taxus baccata* L.) and spruce (*Picea abies* [L.] Karst.) in the radial-tangential and tangential-radial crack propagation system by a micro wedge splitting test

Daniel Keunecke[1,*], Stefanie Stanzl-Tschegg[2] and Peter Niemz[1]

[1] Institute for Building Materials (Wood Physics Group), ETH Zurich, Zurich, Switzerland

[2] Institute of Physics and Materials Science, BOKU, Vienna, Austria

*Corresponding author.
Institute for Building Materials (Wood Physics Group), ETH Zurich, Schafmattstrasse 6, 8093 Zurich, Switzerland
E-mail: danielk@ethz.ch

Abstract

Common yew (*Taxus baccata* L.) and Norway spruce (*Picea abies* [L.] Karst.) are gymnosperm species that differ in their microscopic structure and mechanical characteristics. Compared to spruce, the density of yew wood is high, but the modulus of elasticity is low when loaded parallel to the grain. Information about the transverse load direction is largely lacking. Therefore, the goal of this study was to assess the elastic and fracture mechanical behaviour of both wood species in the radial-tangential plane (crack opening mode I). For this purpose, micro wedge splitting tests were performed. Characteristic elastic and fracture parameters (initial slope, critical load, specific fracture energy) were determined. After the tests, the fracture surfaces were evaluated using microscopic methods. The results reveal clear differences between the species regarding microscopic fracture phenomena and prove that yew wood was significantly stiffer than spruce wood. We suggest that the density and the cell geometry are predominantly responsible for both elasticity and failure behaviour in the transverse direction.

Keywords: fibre bridging; fracture perpendicular to the grain; spruce (*Picea abies*); wedge splitting test; yew (*Taxus baccata*).

Introduction

Interestingly, literature references indicate that common yew is distinctive among gymnosperms in terms of its longitudinal modulus of elasticity (MOE_L). Despite its comparatively high density (~0.62–0.72 g cm^{-3} at 11–12% equilibrium moisture content), the MOE_L of yew is relatively low. Most literature references report values between 6300 and 12,000 MPa (Sekhar and Sharma 1959; Jakubczyk 1966; Wagenführ 2000). This unusual combination prompted us to investigate the elasto-mechanical and fracture-mechanical behaviour of yew wood. Using three-point bending tests, we confirmed the low stiffness (~9000–10,000 MPa) and also observed high axial fracture strain for yew (Keunecke et al. 2006). Our current investigations suggest that a relatively large microfibril angle (MFA), in particular, is the cause of this remarkable mechanical behaviour. Contrary to the stiffness, the longitudinal strength and hardness of yew are of the order of magnitude expected in light of its high density.

However, no data are available for yew from tests with forces acting perpendicular to the grain. Therefore, we tried to bridge this knowledge gap for yew. In a previous study by our group (Märki et al. 2005), the fracture toughness K_{IC} of yew was found to be 0.56 MPa $m^{1/2}$ in the RL orientation and 0.46 MPa $m^{1/2}$ in the TL orientation (the first letter indicates the load direction; the second gives the direction of crack propagation). In a further study, we approximated the stiffness of yew wood by dynamic measurements (ultrasonic waves). We found that yew was 2.3-fold stiffer in the radial direction and 2.0-fold stiffer in the tangential direction compared to spruce (Keunecke et al. 2007).

The present study focuses on the RT and TR orientations. In industrial practice, these orientations play a role, for example, in the defibration procedure and in peeling of veneer logs. Besides elasto-mechanical properties, we wanted to place an emphasis on the fracture mechanical properties and failure characteristics of yew in the transverse plane using a micro wedge splitting test and microscopic methods.

A special wedge splitting method was developed by Tschegg (1986) to determine fracture mechanical values for inhomogeneous materials such as asphalt, concrete and wood. A comprehensive description of the method and its application to wood is given by Stanzl-Tschegg et al. (1995). The splitting device used in this study is a modified version developed by Frühmann et al. (2003) to test comparatively small specimens and to observe the fracture process *in situ* in an environmental scanning electron microscope (ESEM). We used the same equipment for two essential reasons:

1. In contrast to many other test procedures, the specimen geometry is particularly suitable for loading perpendicular to the grain; the equipment and specimen geometry support stable crack propagation.
2. The investigation of relatively small specimens is especially advantageous for yew wood, since this species is characterised by numerous weak points such as knots, grain deviation and irregularities in the

growth ring structure. These sources of errors can be minimised in the case of smaller specimens. Compared to the small specimen dimensions, a relatively large ligament length is given.

Primarily, we wanted to ascertain how the high density and the high percentage of ray cells of yew influence its elastic and fracture mechanical behaviour. As a reference, spruce wood was investigated using the same methodology. The structure of spruce is very different from that of yew. Characteristic elasto-mechanical and fracture parameters were derived from load-displacement curves. Data evaluation was based on the principles of linear elastic fracture mechanics (LEFM) (such as initial stiffness and critical load) and of the fracture energy concept (specific fracture energy). Microscopic fracture phenomena, such as crack paths and fracture surfaces, were evaluated after the tests.

Materials and methods

Micro wedge splitting tests were performed on yew (*Taxus baccata* L.) and spruce wood (*Picea abies* [L.] Karst.). The specimens were oriented in the RT and TR crack propagation directions (crack opening mode I).

For specimen production, five stems each of yew and spruce were chosen from stands in and close to Zurich (Uetliberg region, Switzerland). The green wood was cut to 5-cm-thick planks with a frame saw. After several months of air seasoning, the planks reached a moisture content (MC) of approximately 15–17% and were further dried in a climate chamber at 20°C and 65% RH until the equilibrium MC was reached. For both wood species, a total of 16 slats with a cross-section of 26 mm×30 mm were sawn from the heartwood of the planks taken at breast height. Eight slats each were assigned to the preparation of TR and RT specimens. A series of eight specimens was cut from each wood slat (Figure 1) and stored again at 20°C and 65% RH.

The specimen geometry and dimensions are shown in Figure 2. The starter notch (1 mm wide) was extended using a razor blade to produce as sharp a crack tip as possible. Rounded corners proved to be suitable for avoiding crack initiation in this part of the specimen.

The principle of the micro testing machine for wedge splitting tests according to Frühmann et al. (2003) is presented in Figure 2. A loading head (mounted on a load cell) generates a force *F* on the specimen, causing splitting along the plane of the notch.

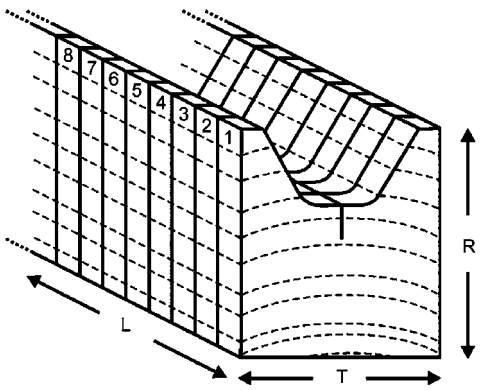

Figure 1 Principle of a series composition (in this example, oriented in the TR crack propagation direction): eight adjacent specimens were sawn from each wood slat.

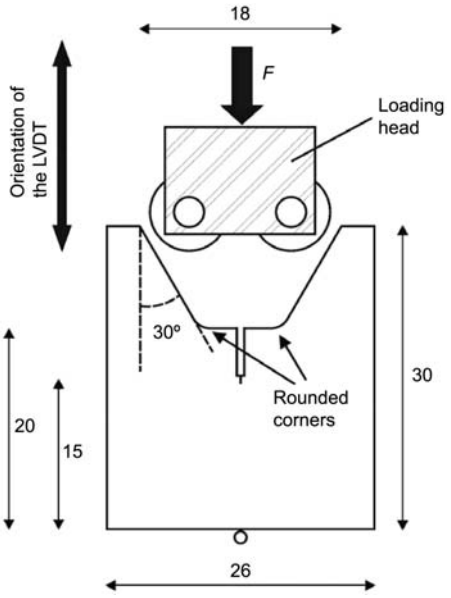

Figure 2 Scheme of the experimental set-up with the loading head and a specimen (all dimensions in mm). The specimens are 4 mm thick and supported below by a bearing.

To reduce friction to a minimum, the force is transmitted to the specimen through roller bearings. The force comprises a large horizontal force (mode I load) and a small vertical force. The latter is too small to affect the fracture behaviour of the samples.

The contact force is measured by the load cell. The bottom end of the specimen is supported by a bearing pin that allows the broken halves to move apart. The vertical displacement of the loading head was measured by a linear variable differential transformer. The displacement-controlled loading rate was 6 μm s^{-1}. Tests were performed *ex situ* in a climate chamber under standard climatic conditions (20°C and 65% RH) at sample equilibrium MC. After the tests, the crack paths and further fracture phenomena of selected specimens were evaluated using a LEO 435 VPi scanning electron microscope (SEM) and an Olympus SZX9 stereo microscope. The small specimen thickness guaranteed that surface observations were representative of the behaviour of the interior of the specimen.

Results and discussion

Characteristic elasto-mechanical and fracture parameters such as initial stiffness, critical load and specific fracture energy were calculated based on the load-displacement responses obtained from the experiments. Following the approach of Frühmann et al. (2003), neither pure opening mode I forces (horizontal splitting force) nor horizontal displacement (corresponding to the crack mouth opening displacement) were calculated from the recorded load/displacement data, since explicit knowledge of these is not required for evaluation of the specific fracture energy.

All of the parameters discussed below were determined for each specimen in a series and subsequently averaged for each series (the statistical scatter within each series was small). This means that only the series were compared for evaluation, rather than single specimens. In the case of TR orientation, specimens were tested in both crack propagation directions, from pith to bark and vice versa. Since no significant differences

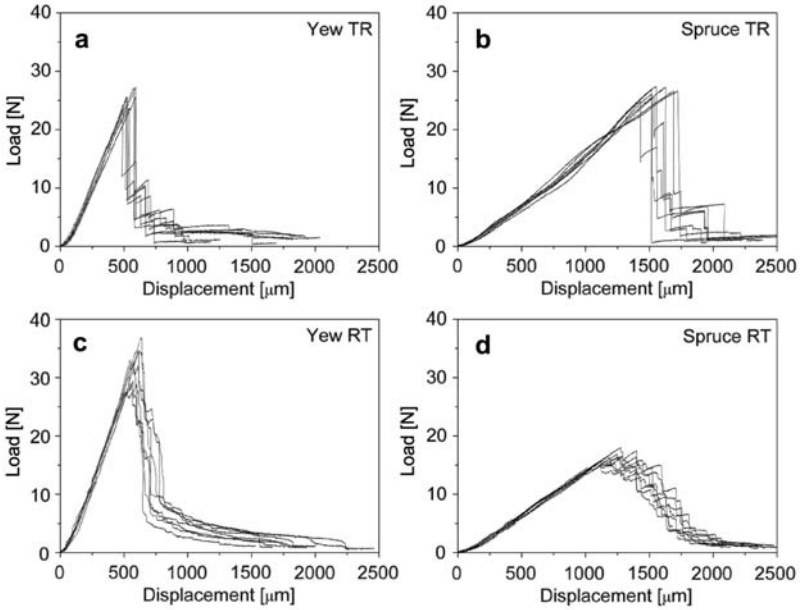

Figure 3 Load-displacement diagrams of representative test series: (a) yew TR, (b) spruce TR, (c) yew RT and (d) spruce RT. "Displacement" represents the vertical displacement of the loading head. The reason for the slight kink in the slope of graph (b) is unclear and was not present in the other graphs.

between the two groups were found regarding the fracture parameters and crack propagation, we did not distinguish between the directions in the following. Diagrams of representative series of both wood species and crack propagation systems are shown in Figure 3.

Characteristic behaviour prior to the load peak

Initial stiffness The first phase of the load-displacement graph is characterised by linear elastic response. The initial slope k_{init} corresponds to the stiffness of a material and is proportional to an effective modulus of elasticity (Harmuth et al. 1996). No significant differences were found between the RT and TR orientations for both species; k_{init} was only slightly higher for yew RT than for yew TR, whereas it was distinctly higher for spruce TR than for spruce RT (Table 1). Comparison between the species showed that k_{init} was four-fold greater for yew than for the clearly less dense spruce specimens. In other words, yew is much stiffer than spruce when loaded perpendicular to the grain.

In preliminary three-point bending tests (Keunecke et al. 2006) and tensile tests spruce had a slightly higher MOE than yew for force parallel to the grain. The dependence on the load direction can be ascribed to the fact that wood is a type of cellular (honeycomb-like) material in the transverse direction, whereas it has a fibrous structure in the longitudinal direction (length/diameter ratios are between 30:1 and 100:1) (Frühmann et al. 2003). The stretchability in the R and T directions depends on the cell wall/lumen ratio and the density. As a result, the initial slope k_{init} in both crack propagation systems strongly correlated with the density measured for the specimens. Linear regression indicated high significance with correlation coefficients of R = 0.92 for yew RT, R = 0.87 for yew TR, R = 0.97 for spruce RT, and R = 0.73 for spruce TR.

In contrast to transverse stretching, longitudinal stretching requires extension of the cell walls. Therefore,

Table 1 Characteristic results of the wedge splitting tests.

	ρ (kg m^{-3})	k_{init} (N μm^{-1})	F_{crit} (N)	s_{crit} (μm)	F_{max} (N)
Yew RT					
Mean	640	0.063	31.3	567	32.4
CoV (%)	9.7	13.4	13.8	4.6	15.2
Yew TR					
Mean	600	0.059	25.0	542	25.4
CoV (%)	7.7	13.6	10.9	9.3	11.4
Spruce RT					
Mean	450	0.015	17.2	1216	17.6
CoV (%)	5.7	22.5	13.6	8.4	13.4
Spruce TR					
Mean	470	0.017	23.2	1559	24.4
CoV (%)	5.0	18.0	13.2	11.5	7.3

Data presented are mean values for eight experiments. CoV, coefficient of variation; RT, radial-tangential; TR, tangential-radial; ρ, raw density; k_{init}, initial slope of the load-displacement graph; F_{crit}, critical load (end of the linear elastic phase in the load-displacement graph); s_{crit}, displacement corresponding to F_{crit}; F_{max}, maximum load.

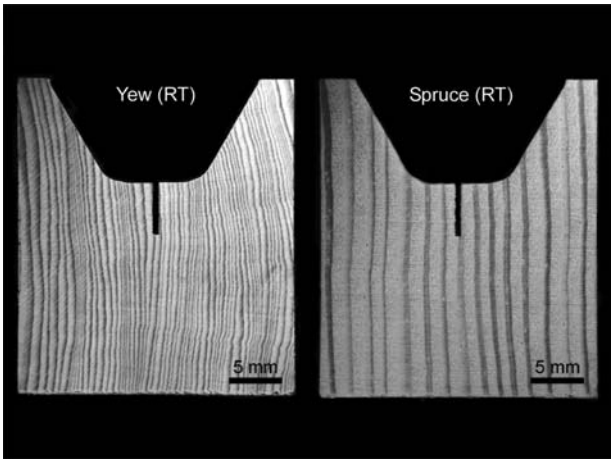

Figure 4 Different ring widths of yew and spruce.

longitudinal elasticity largely depends on MFA of the helically oriented cellulose fibrils in the thickest tracheid cell wall layer S2 (Reiterer et al. 1999), whereas the S2 MFA does not influence the transverse elasticity of the fibre wall (Bergander and Salmen 2000). Thus, a wood species with a large MFA (typical for yew) and relatively thick cell walls can be relatively deformable in the axial direction (i.e., low MOE and high fracture strain) and rigid in the transverse direction at the same time. Moreover, the narrow growth rings of yew wood (Figure 4) lead to a greater influence of the stiffer latewood (LW) tracheids and to a more homogeneous stress distribution between zones of earlywood (EW) and LW. It should be considered, however, that the stress distribution in a notched specimen (as was the case in this study) is different from that in an unnotched specimen in a uniaxial load case, where the stress is not concentrated around the notch tip, but evenly distributed across the cross-sectional area of the sample.

Critical load According to Frühmann et al. (2003), the critical load F_{crit} represents the end of the linear elastic phase and therefore indicates macro-crack initiation. F_{crit} is proportional to the critical stress intensity factor K_{IC} in the LEFM theory. Since the distance between the notch tip and the line of the acting horizontal force decreased during the tests, K_{IC} could not be calculated directly.

Mean values of the critical load are higher for yew than for spruce (Table 1); the corresponding displacement s_{crit} is approximately 2.5- to three-fold greater for the more compliant spruce. The maximum load F_{max} is not markedly higher than the crack initiation load; in many cases it is even identical.

Material stiffness and strength perpendicular to the grain vary with load orientation, as well as density. Typically, both MOE (Keunecke et al. 2007) and strength [e.g., $K_{IC(RL)} > K_{IC(TL)}$; Märki et al. 2005] of yew and spruce are higher in the radial than in the tangential direction. This could be confirmed for yew specimens in this study (F_{crit} RT = 31.3 N, F_{crit} TR = 25.0 N). The radial reinforcement of wood tissue by means of wood rays (Burgert et al. 1999) is one of several effects contributing to this anisotropy. Yew wood is characterised by a relatively high percentage of ray cells (~14%) compared to spruce (~5%) (Wagenführ 2000). For spruce specimens, however, F_{crit} is lower in the RT (17.2 N) than in the TR (23.2 N) orientation, which is in accordance with the slightly higher initial stiffness of spruce in the TR direction (see above).

Even though this relationship may not be generally valid for spruce considering the high variation, a combination of size effects and the test procedure for prenotched specimens could explain the result. The sharp crack tip position in particular may play a major role. From the beginning of the test up to the critical load, the crack does not propagate and a process zone develops around the crack tip. The greatest concentrations of stress occur directly in front of the tip. As the tip was located in the EW zone of spruce RT specimens in most cases (which is wide compared to the narrow yew EW zones), it is likely that predominantly fracture parameters of the EW zone were determined. The density, namely the cell wall/lumen ratio, is clearly higher for yew in both EW and LW (Table 2). Furthermore, the density gradient between EW and LW is smaller for yew than for spruce. In other words, EW zones of spruce are more pronounced planes of weakness compared to the relatively compact EW zones of yew wood. The latter are also reinforced by more rays. Consequently, F_{crit} is nearly twice as high for yew in the RT direction.

Characteristic behaviour beyond the load peak

TR specimens After passing the critical load (at which initiation of the macro-crack takes place), a first sudden decrease occurs in the load-displacement curve. During this first decrease, the crack propagates across one or several tree-ring boundaries and stops again in an EW zone. This was visible even to the naked eye. When the crack stops, the load increases to a new local maximum before it decreases again, accompanied by further crack propagation. These stepwise increases and decreases usually repeat several times (Figure 3a,b), with the slope of each subsequent increase being less steep than the

Table 2 Tracheid dimensions of yew and spruce wood (Wagenführ 2000). Order of listing: minimum, mean, maximum.

	Yew			Spruce		
Length (μm)	1550	1950	2250	1300	2800	4300
Lumen diameter (μm)						
EW	12.1	18.4	27.8	16.0	32.0	45.0
LW	5.1	9.4	14.3	6.4	17.4	22.0
Wall thickness (μm) (double cell wall)						
EW	3.3	4.2	5.4	1.9	3.5	4.9
LW	6.8	7.7	9.7	9.3	10.7	11.6

EW, earlywood; LW, latewood.

previous one. Future investigations should demonstrate whether this unstable crack propagation in the TR orientation can be avoided if a modified electronic control loop with a quicker response time is available.

Softwood tracheids are predominantly arranged in straight lines in the radial direction. The crack path typically followed interfaces between rays and tracheids, which are well known as planes of weakness. Owing to the high cell wall/lumen ratios, only intercellular fracture (separation of cells along their middle lamella) was observed for yew in both EW (Figure 5a) and LW zones, as well as for spruce in LW (Figure 5b) zones. In spruce EW, both intercellular and transwall fracture occurred (Figure 5b), the latter in the tangentially oriented part of the tracheid walls.

Yew and spruce clearly differed regarding the development of fibre bridging, the principle of which is schematically shown in Figure 6. In the case of spruce, only a few partially delaminated tracheids (if any) bridged the gap in the immediate vicinity of the crack tip. In the study of Frühmann et al. (2003), fibre bridging was even completely lacking for spruce TR specimens. In contrast, yew specimens featured a high degree of fibre bridging, partly spanning the complete gap behind the crack tip (Figure 7a). This characteristic, combined with the narrow growth rings of yew, possibly prevents abrupt crack propagation and results in a failure process with more intermediate steps (Figure 3a).

RT specimens Contrary to the clearly unstable crack propagation in the TR orientation, crack growth in RT specimens was characterised by both stable and unstable phases of propagation (Figure 3c,d). In other words, short-term phases of arrest sometimes occurred before the crack continued propagating. This more stable behaviour in the RT orientation is due to the fact that no sudden obstacle (such as LW bands in TR specimens) forces the crack to pause. However, it is conceivable that rays temporarily delay crack propagation, although less effectively than LW bands.

After the peak load, quasi-brittle materials with stable crack propagation ideally form a strain-softening region (decreasing load values) with a smooth curve progression in the load-displacement graph. Only few specimens of

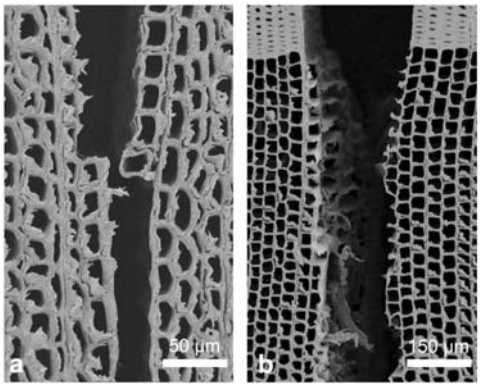

Figure 5 Crack paths in TR orientation of yew earlywood (a) and spruce (b): predominant intercellular fracture of yew (a) and in latewood of spruce (b) and predominant cell wall fracture in earlywood of spruce (b).

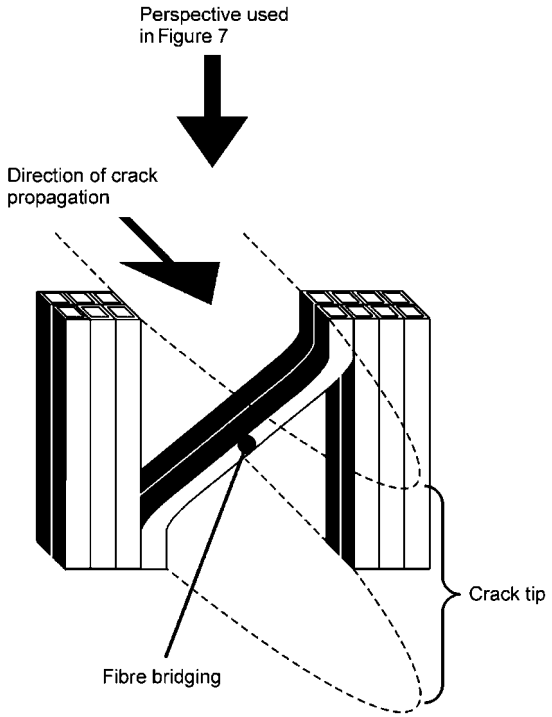

Figure 6 Principle of fibre bridging if the crack is oriented in the RT or TR crack propagation system.

the RT series behaved approximately like this (Figure 8) and therefore could be used to calculate the specific fracture energy G_f according to Eq. (1). G_f is the non-linear counterpart of the critical strain energy release rate G_c and indicates the total energy consumed by crack initiation and crack propagation. G_f corresponds to the area integrated over the load-displacement curve divided by the nominal fracture surface area A (A = ligament length multiplied by specimen thickness):

$$G_f = \frac{1}{A}\int_0^{s_{end}} F(s)\cdot ds, \qquad (1)$$

where $F(s)$ is the force measured by the load cell and s is the vertical displacement of the loading head. The specimen dimensions are too small to eliminate a size

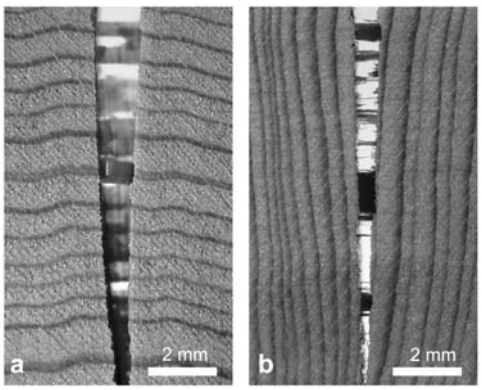

Figure 7 Fibre bridging in yew specimens tested in the TR (a) and RT (b) orientation: the samples are positioned in front of a bright background. The dark zones between both specimen halves are tracheids "bridging" the gap behind the crack tip (see also Figure 6).

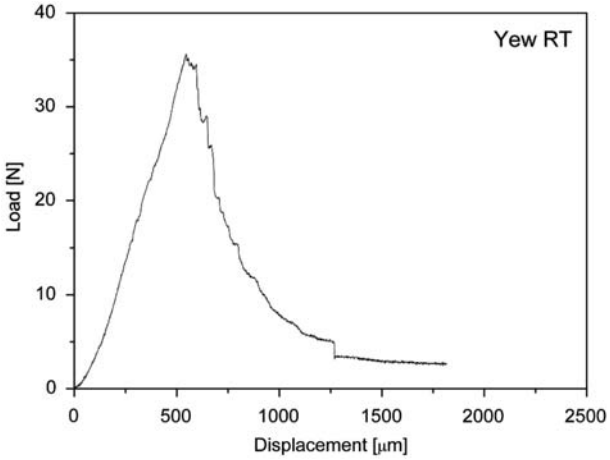

Figure 8 Stable crack propagation in a yew RT specimen.

effect on G_f according to earlier studies (Stanzl-Tschegg et al. 1995). The fracture process zone is probably not completely covered by the specimen size. Although transfer of our results to larger dimensions might include a certain error, direct comparison between two species with the same specimen geometry is legitimate.

The results in Table 3 are based on a reduced number of samples, namely five yew and eight spruce series, with three to four specimens per series showing stable crack propagation. Therefore, the mean values and coefficients of variation for density deviate from those in Table 1. The high strength of yew specimens is compensated by the higher compliance (higher displacement s_{crit}) of spruce specimens. This leads to similar specific fracture energies for both wood species. It must be noted, however, that the statistical spread of G_f is rather high for yew (32.4%).

Tschegg et al. (2001) determined crack initiation energy (G_{init}) and crack propagation energy (G_{prop}) separately. For the following reason, this distinction was not possible in our study: G_{init} is defined as the area under the load-displacement curve from the origin to the peak, and back down a line running parallel to the initial slope of the curve. G_{prop} is the difference between the total specific fracture energy (G_f) and G_{init}. In our study, a non-linear region prior to the peak was often lacking. The maximum load was therefore visible as a sharp peak directly subsequent to the linear elastic range (Figure 8). Thus, calculation of G_{init} was not feasible since G_{init} was almost zero.

Cracks always take the path of least resistance, i.e., in the RT orientation, they usually propagate in EW. Since tracheids are arranged irregularly in the tangential direction, the crack path is not as straight as observed for TR specimens (Figure 9). In spruce specimens, cell wall fracture of the thin, radially oriented EW tracheid walls was the dominant failure mechanism (Figure 9a); intercellular fracture was also present, but clearly less frequently. In contrast, only intercellular fracture was observed in yew specimens (Figure 9b) owing to the strong design of EW tracheids. In some cases, the crack path temporarily changed from the EW to the LW zone, crossed the growth ring boundary and continued propagation in the EW zone of the neighbouring tree ring. On the one hand, this behaviour of yew specimens might result from the relatively small density gradient between EW and LW (Table 2) and the resultant intercellular fracture. On the other hand, the probability that a crack propagates exclusively in EW decreases when the growth rings are extremely narrow. In the case of yew, it is likely that more growth rings are covered by the process zone.

As described above for TR specimens, fibre bridging in RT specimens is clearly more pronounced for yew than for spruce (Figure 7b). This crack closure mechanism obviously plays a major role for yew in dissipating energy in both the radial and tangential crack propagation phases. According to Vasic and Smith (2002), fibre bridging is the main fracture toughening mechanism. Once mobilised near the crack tip, it causes energy to be dissipated more gradually, as found for yew in both crack propagation orientations. Reiterer et al. (2002) assumed that fibre bridging was more effective in spruce than in hardwoods, since spruce tracheids are longer. As yew tracheids are shorter than those of spruce, our results do not confirm this hypothesis, i.e., tracheid length alone cannot be the decisive criterion for the formation of fibre bridging. Pre-existing micro-cracks can also contribute to fracture toughening in the zone in which non-linear strain-softening fracture takes place. Although we did not observe any micro-cracks, they are likely to be present in all wooden specimens and their perception is only a question of magnification. The exact nature of energy

Table 3 Fracture energy results.

	ρ (kg m^{-3})	G_f (N mm^{-1})
Yew RT		
Mean	630	0.31
CoV (%)	11.5	32.4
Yew TR	–	–
Spruce RT		
Mean	450	0.29
CoV (%)	5.9	3.5
Spruce TR	–	–

Data presented are mean values for five yew and eight spruce experiments with three to four specimens per experiment. CoV, coefficient of variation; RT, radial-tangential; TR, tangential-radial; ρ, raw density; G_f, specific fracture energy; –, no stable crack propagation.

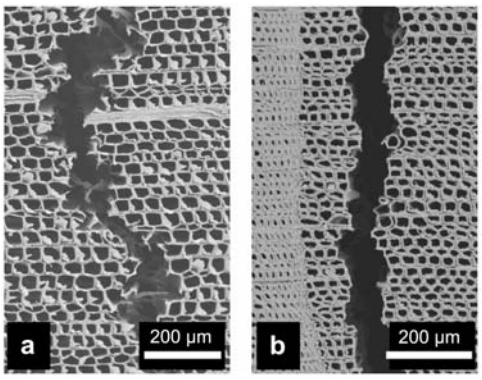

Figure 9 Crack paths in RT orientation of spruce (a) and yew (b).

dissipation in the fracture process zone is still a matter of discussion (Smith et al. 2003).

Conclusions

The micro wedge splitting test proved to be suitable for characterising the fracture and fracture mechanical parameters of yew and spruce specimens in the transverse plane. Differences between the species regarding fracture behaviour were ascribed to variability of microstructural features such as the cell wall/lumen ratio and the density gradient between EW and LW. Yew specimens, with high density and a high percentage of ray cells, were stiffer and stronger than spruce. During crack propagation, mainly intercellular fracture occurred in yew, whereas transwall fracture was also present in spruce EW. The specific fracture energy in RT-oriented specimens was similar for both species, since the higher strength of yew and the higher compliance of spruce cancelled each other out.

In conclusion, our study revealed that a wood species can be compliant in the axial and rigid in the transverse direction at the same time. In preliminary tests, a relatively low MOE was found for yew when a force was acting in the longitudinal direction. The literature indicates that yew is well known for its high toughness. Pronounced fibre bridging might contribute to this characteristic property, since it is an important toughening mechanism for dissipating energy during crack propagation. The crack initiation and propagation process will be studied further *in situ* using ESEM equipment.

Acknowledgements

This work was supported by European Cooperation in the field of Scientific and Technical research (COST Action E35) for a short-term scientific mission (STSM) stay by D. Keunecke at the Institute of Physics and Materials Science at BOKU University, Vienna.

References

Bergander, A., Salmen, L. (2000) Variations in transverse fibre wall properties: Relations between elastic properties and structure. Holzforschung 54:654–660.

Burgert, I., Bernasconi, A., Eckstein, D. (1999) Evidence for the strength function of rays in living trees. Holz Roh Werkst. 57:397–399.

Frühmann, K., Burgert, I., Stanzl-Tschegg, S.E., Tschegg, E.K. (2003) Mode I fracture behaviour on the growth ring scale and cellular level of spruce (*Picea abies* [L.] Karst.) and beech (*Fagus sylvatica* L.) loaded in the TR crack propagation system. Holzforschung 57:653–660.

Harmuth, H., Rieder, K., Krobath, M., Tschegg, E. (1996) Investigation of the nonlinear fracture behaviour of ordinary ceramic refractory materials. Mater. Sci. Eng. A Struct. 214:53–61.

Jakubczyk, B. (1966) Technical properties of the yew wood from the preserve Wierzchlas. Sylwan 10:79–86.

Keunecke, D., Märki, C., Niemz, P. (2006) Selected mechanical properties and fracture characteristics of yew wood. In: Fracture of Nano and Engineering Materials and Structures. Ed. Gdoutos, E.E. Springer, Dordrecht. pp 1189–1190.

Keunecke, D., Sonderegger, W., Pereteanu, K., Lüthi, T., Niemz, P. (2007) Determination of Young's and shear moduli of common yew and Norway spruce by means of ultrasonic waves. Wood Sci. Technol. 41:309–327.

Märki, C., Niemz, P., Mannes, D. (2005) [Comparative studies on selected mechanical properties of yew and spruce]. Schweiz. Z. Forstwes. 156:85–91 (in German).

Reiterer, A., Lichtenegger, H., Tschegg, S., Fratzl, P. (1999) Experimental evidence for a mechanical function of the cellulose microfibril angle in wood cell walls. Philos. Mag. A 79:2173–2184.

Reiterer, A., Sinn, G., Stanzl-Tschegg, S.E. (2002) Fracture characteristics of different wood species under mode I loading perpendicular to the grain. Mater. Sci. Eng. A Struct. 332: 29–36.

Sekhar, A.C., Sharma, R.S. (1959) A note on mechanical properties of *Taxus baccata*. Indian For. 85:324–326.

Smith, I., Landis, E., Gong, M. Fracture and Fatigue in Wood. Wiley, Chichester, 2003.

Stanzl-Tschegg, S.E., Tan, D.M., Tschegg, E.K. (1995) New splitting method for wood fracture characterisation. Wood Sci. Technol. 29:31–50.

Tschegg, E.K. (1986) [Equipment and appropriate specimen shape for test to measure fracture values]. Patent AT-390328 (in German).

Tschegg, E.K., Frühmann, K., Stanzl-Tschegg, S.E. (2001) Damage and fracture mechanisms during mode I and III loading of wood. Holzforschung 55:525–533.

Vasic, S., Smith, I. (2002) Bridging crack model for fracture of spruce. Eng. Fract. Mech. 69:745–760.

Wagenführ, R. Holzatlas. Fachbuchverlag Leipzig, München, 2000.

Received December 20, 2006. Accepted May 22, 2007.
Published online July 9, 2007.